Brain Structure and Function (2021) 226:801–816
https://doi.org/10.1007/s00429-020-02210-7

ORIGINAL ARTICLE

Speech rate association with cerebellar white-matter diffusivity in adults with persistent developmental stuttering

Sivan Jossinger[1] · Vered Kronfeld-Duenias[1] · Avital Zislis[1] · Ofer Amir[2] · Michal Ben-Shachar[1,3]

Received: 30 June 2020 / Accepted: 22 December 2020 / Published online: 4 February 2021

Abstract

Speech rate is a basic characteristic of language production, which affects the speaker's intelligibility and communication efficiency. Various speech disorders, including persistent developmental stuttering, present altered speech rate. Specifically, adults who stutter (AWS) typically exhibit a slower speech rate compared to fluent speakers. Evidence from imaging studies suggests that the cerebellum contributes to the paced production of speech. People who stutter show structural and functional abnormalities in the cerebellum. However, the involvement of the cerebellar pathways in controlling speech rate remains unexplored. Here, we assess the association of the cerebellar peduncles with speech rate in AWS and control speakers. Diffusion MRI and speech-rate data were collected in 42 participants (23 AWS, 19 controls). We used deterministic tractography with Automatic Fiber segmentation and Quantification (AFQ) to identify the superior, middle, and inferior cerebellar peduncles (SCP, MCP, ICP) bilaterally, and quantified fractional anisotropy (FA) and mean diffusivity (MD) along each tract. No significant differences were observed between AWS and controls in the diffusivity values of the cerebellar peduncles. However, AWS demonstrated a significant negative association between speech rate and FA within the left ICP, a major cerebellar pathway that transmits sensory feedback signals from the olivary nucleus into the cerebellum. The involvement of the ICP in controlling speech production in AWS is compatible with the view that stuttering stems from hyperactive speech monitoring, where even minor deviations from the speech plan are considered as errors. In conclusion, our findings suggest a plausible neural mechanism for speech rate reduction observed in AWS.

Keywords DTI · Tractography · Speech-rate · Articulation rate · Stuttering · Cerebellum

Introduction

The production of speech is a multifaceted process that requires the integration of diverse sources of information, including efficient lexical search and access, motor and articulatory programming, somatosensory feedback and respiratory coordination (Guenther 2006). A basic characteristic of speech production is speech rate, affecting speakers' intelligibility, fluency, and communication efficiency. Beyond its role in everyday communication, speech rate is also a key factor in the clinical assessment of various speech disorders, such as apraxia of speech (Kent and Rosenbek 1983), dysarthria (Kent et al. 1987), and persistent developmental stuttering. In adults who stutter (AWS), speech rate is usually slower compared to fluent speakers, and correlated with stuttering severity, even when speech rate is assessed solely based on fluent utterances (de Andrade et al. 2003; Ingham et al. 2012; Kell et al. 2009). Here, we investigate the neural

Supplementary Information The online version contains supplementary material available at https://doi.org/10.1007/s00429-020-02210-7.

✉ Sivan Jossinger
sivanyoss@gmail.com

✉ Michal Ben-Shachar
michalb@mail.biu.ac.il

[1] The Gonda Multidisciplinary Brain Research Center, Bar-Ilan University, Ramat-Gan, Israel

[2] Department of Communication Disorders, Sackler Faculty of Medicine, Tel-Aviv University, Tel-Aviv, Israel

[3] Department of English Literature and Linguistics, Bar-Ilan University, Ramat-Gan, Israel

pathways that are associated with speech rate in both AWS and fluent speakers.

To enable the complex task of speech production, speakers utilize a large network of cortical and subcortical brain regions (Bohland and Guenther 2006; Hickok 2012; Tourville and Guenther 2013; Tremblay et al. 2016). Broadly, motor control of speech production relies on a distributed neural system of distant brain regions which are wired through several cortico-striatal-thalamic and cortico-cerebellar-thalamic loops (Bohland and Guenther 2006; Tremblay et al. 2016). Within this network, the cerebellum seems to play a cardinal role in mediating speech rate. Indeed, fMRI studies of syllable repetition at different rates (2–6 Hz) found that the hemodynamic response in the cerebellum displays a stepwise increase of activation between 3 and 4 Hz (Riecker et al. 2005, 2006). This suggests that cerebellar control may be engaged in speech rates higher than 3 Hz. In line with this view, patients with cerebellar ataxia have been repeatedly shown to have reduced speech rate, approaching 3 Hz, compared to healthy subjects whose speech rate varies around 4.95 Hz, as measured during syllable repetition (Ackermann and Brendel 2016; Schalling and Hartelius 2013). Despite the extensive work on cerebellar contribution to speech rate, little is known about the unique contribution of the cerebellar white matter pathways to this component.

The fibers that carry the cerebellar input and output information converge into three major white matter pathways: the superior cerebellar peduncle (SCP), the middle cerebellar peduncle (MCP), and the inferior cerebellar peduncle (ICP) (Perrini et al. 2013). The SCP is mainly composed of efferent fibers that carry signals from the deep cerebellar nuclei to the contralateral cortex via the thalamus. The MCP is mainly composed of afferent fibers carrying signals from the cerebral cortex to the contralateral cerebellar cortex. Finally, the ICP is mainly composed of afferent fibers feeding signals from the spine and the olivary nucleus into the ipsilateral cerebellar cortex (Perrini et al. 2013). Functioning as exclusive bridges between the cerebellum and extra-cerebellar regions, the structural properties and organization of the cerebellar peduncles (CPs) are important for understanding the neural basis of speech rate.

Speech rate is implicated in various speech disorders, including developmental stuttering. It has been proposed that aberrant speech rate is associated with the onset, development, and maintenance of stuttering. The pre-onset speaking rate of children who stutter is faster compared to their fluent peers (Kloth et al. 1995), while children who recovered from stuttering exhibit slower speech rate compared to those whose stuttering persisted (Hall et al. 1999). In adults who stutter, slower speech rate is commonly observed compared to fluent speakers (de Andrade et al. 2003; Kell et al. 2009). Furthermore, speech rate modification approaches have been shown to facilitate fluency in AWS (Adams et al. 1973). Although the reduced speech rate among people who stutter can be partly explained by the time spent on disfluent utterances, experimental data show that AWS exhibit slower speech even during fluent epochs[1] (Ingham et al. 2012; Zimmermann 1980b).

Many view stuttering as a pathology of the motor control system (Alm 2004; Civier et al. 2010; Dietz et al. 1994; Max et al. 2004; Watkins et al. 2015, 2007; Zimmermann 1980a, b, c). Models of speech motor control propose that the ability to produce rapid, fluent speech is dependent on an internal representation of the predicted auditory consequence following a specific articulatory motor plan (Guenther 2006; Hickok 2012). In line with that perspective, it has been proposed that an impairment in this "internal model" might cause speech deficits that resemble stuttering, including slowed speech rate (Civier et al. 2010; Max et al. 2004). Accumulative data attribute the computation of internal models to the cerebellum (Wolpert et al. 1998). Nevertheless, the direct link between stuttering, speech rate, and the cerebellum was not investigated to date.

Neuroimaging studies suggest altered connectivity in AWS across widely distributed locations within their speech production network (Cai et al. 2014; Chang et al. 2011; Cieslak et al. 2015; Connally et al. 2014; Kronfeld-Duenias et al. 2016a, 2016b; Lu et al. 2012; Neef et al. 2018; Sitek et al. 2016; Xuan et al. 2012; Yang et al. 2016). Diffusion MRI (dMRI) studies detected stuttering-related microstructural differences in several of the white matter pathways that are presumably involved in motor aspects of speech production. For example, recent studies by our group and others identified group differences between AWS and controls in the frontal aslant tract (FAT), connecting the inferior frontal gyrus with the supplementary motor area (Kronfeld-Duenias et al. 2016a; Neef et al. 2018). The critical role of the FAT in stuttering is further supported by results showing that direct axonal stimulation of this tract evokes stuttering-like dysfluencies (Kemerdere et al. 2016). Microstructural group differences between people who stutter and fluent speakers were further detected in the corticospinal tract (CST), connecting the primary motor cortex and the spinal cord (Cai et al. 2014; Chang et al. 2008). While other pathways have also been implicated in developmental stuttering, this general pattern of findings suggests that motor control pathways may provide an important key for understanding speech control in stuttering.

Along these lines, cerebellar differences were detected in several studies comparing people who stutter and fluent

[1] Speech rate during fluent epochs is typically defined as 'articulation rate'. While this is the more precise technical term for the measure we calculated, the term speech rate is maintained throughout the paper for the sake of simplicity.

speakers using functional and structural imaging methods. For example, functional studies report elevated cerebellar activity in AWS (De Nil et al. 2003), an abnormal integration of information across the cerebellum-premotor circuit of AWS (Lu et al. 2009), and a positive correlation between speech rate and cerebellar activity among AWS (Fox et al. 2000). With respect to the cerebellar white matter structure, decreased fractional anisotropy values were found in both children who stutter (Chang et al. 2015) and AWS (Connally et al. 2014). Specifically, using an ROI-based approach, Connally et al. (2014) showed that AWS have reduced FA in all CPs compared to fluent controls. The structural differences in the CPs, together with the involvement of the cerebellum in controlling speech rate, suggest an indirect relation between speech rate and the microstructural properties of the CPs among AWS. However, to the best of our knowledge, this is the first study that directly examines the associations between speech rate and structural properties of the CPs in AWS.

In the current study, we evaluated the association between individual speakers' speech rate and diffusivity estimates extracted from their CPs, in both AWS and fluent speakers. Our aims were twofold: (1) To assess previously reported group differences between AWS and controls in the microstructural properties of their CPs, and (2) To evaluate and compare the pattern of association between speech rate and CP-diffusivities in AWS vs. controls. Participants underwent a behavioral assessment to evaluate their stuttering severity and speech rate, and a dMRI scan to allow the structural analysis of their CPs. We identified, in each participant, the SCP, MCP and ICP, bilaterally, and extracted their microstructural properties. We tested for group differences in diffusivity and assessed the association between diffusivity and speech rate, in both AWS and controls. Based on Connally et al. (2014), we expected to find structural group differences in the CPs. Moreover, we hypothesized significant group-differences between AWS and controls in the association patterns observed between speech rate and CP-diffusivity. Specifically, based on fMRI evidence (De Nil et al. 2003), we hypothesized stronger reliance on the cerebellum in controlling speech rate in AWS, and hence a tighter coupling between CP properties and speech rate measures in the experimental group, compared to controls.

Methods

Participants

A total of 44 participants were recruited as part of a larger study (Kronfeld-Duenias et al. 2018). The participants were all Hebrew speakers, physically healthy, with no history of neurological disease or psychiatric disorders. This study was approved by the Helsinki committee of the Tel-Aviv Sourasky Medical Center and by the ethics committee of the Faculty of Humanities at Bar-Ilan University.

Participants were assigned to the AWS group based on three criteria: (1) Self-reported history of stuttering since childhood, (2) displayed more than three stuttered-like disfluencies (SLD, see "Speech measurements"; Ambrose and Yairi 1999) per 100 syllables during an unstructured interview, and (3) Scored at least 10 on the Stuttering Severity Instrument (SSI-3, see "Stuttering severity evaluation") (Riley 1994). The assignment of participants to the control group was based on their self-report of having no history of stuttering. Group assignment was verified by two speech pathologists based on audio and video recordings of an unstructured interview (see "Speaking tasks"). Following the above criteria, 25 participants were assigned to the AWS group (6 females), and 19 participants were assigned to the control group (3 females).

Speaking tasks

Speech evaluation was based on two speaking tests: an unstructured interview and a reading test (Riley 1994). Each session took place in a quiet room. Sessions were recorded simultaneously with a digital video camera (Sony DCR-DVD 106E, Sony Corporation of America, New York, NY, USA) and with a noise-canceling microphone (Sennheiser PC21, Sennheiser Electronic Corporation, Berlin, Germany). Audio signals from the microphone were digitally recorded using audio processing software (Goldwave, Inc., St. John's, Canada) on a mono channel, with a sampling rate of 48 kHz (16 bit).

Unstructured interview

The unstructured interview was used to assess the spontaneous speech rate. Each participant was asked to talk for 10 min about a neutral topic (e.g., a recent travel experience, a movie, a book). The experimenter (V.K.-D.) refrained from interrupting, and only asked questions when the participant was having difficulty to find a topic to talk about.

Reading task

Each participant was asked to read aloud one of three paragraphs from the standardized and phonemically balanced *Thousand Islands* reading passage (Amir and Levine-Yundof 2013). The paragraphs were of similar length (~200 syllables) and were randomly assigned to the participants.

Written semantic fluency task

Participants were requested to write down as many exemplars as they can, within 1 min, for a given semantic category. The task was repeated 3 times, with different semantic categories: animals, fruits and vegetables, and vehicles. A spoken variant of this task was validated and standardized in Hebrew speaking adults (Kavé 2005). Written responses were elicited in our study to avoid the direct effects of disfluencies on individuals' performance. This task served to assess ease of lexical access separately from speech fluency.

MRI data acquisition

MRI scans were performed on a 3 T General Electric MRI scanner at the Tel-Aviv Sourasky Medical Center. The MRI protocol included standard anatomical and diffusion imaging sequences, as detailed below. Functional MRI scans were also included in the scan protocol but are not reported here (see Halag-Milo et al. 2016 for fMRI results in this sample).

T1 image acquisition

High-resolution T1 anatomical images were acquired using a 3D fast spoiled gradient-echo (FSPGR) sequence, with a spatial resolution of $1 \times 1 \times 1$ mm voxel size. We collected about 150 ± 12 axial slices per subject, covering the entire cerebrum and cerebellum.

Diffusion weighted image acquisition

A standard dMRI protocol was applied by means of a single-shot spin-echo diffusion-weighted echo-planar imaging (DW-EPI) sequence (~68 axial slices, 2 mm thick, with no gap; matrix size = 128×128, with a voxel size of $2 \times 2 \times 2$ cubic mm). dMRI data were acquired along 19 non-collinear gradient directions ($b = 1000$ s/mm^2) and one reference volume ($b = 0$ s/mm^2). This protocol was repeated twice for an improved signal-to-noise ratio.

Data analysis

Behavioral data analysis

Speech measurements

Two speech measures were used in the current study: (1) Speech rate, and (2) Stuttered-like disfluencies (SLD). The measures were calculated manually based on the audio recordings of the unstructured interview. As a first step, the interviews were transcribed, and disfluent utterances (such as hesitations, prolongations, repetitions, and pauses longer than 250 ms) were annotated. This was done by two trained research assistants and re-evaluated by an expert speech pathologist (O.A.). To reduce potential bias, both research assistants and the speech pathologist were blind to the participants' group assignment (AWS or control). At the end of this process, a minimum of 600 syllables for each participant was obtained.

Speech rate was calculated as the ratio between the total number of analyzed syllables and the time it took the participants to produce them (i.e., syllables/sec). For the purpose of this study, we calculated speech rate only during fluent utterances, after excluding disfluent speech segments (Ambrose and Yairi 1999; Amir 2016; Amir and Grinfeld 2011; Rochman and Amir 2013). This analysis was performed following the detailed description in Amir and Grinfeld (2011). In short, an utterance was defined based on three criteria: (1) communicated an idea, (2) had a well-defined intonation contour, and (3) was grammatically complete. Utterances that included disfluencies, hesitations, or pauses greater than 250 ms, were manually identified. In such cases, the entire sentence was excluded, to avoid potential effects of the stuttered utterances on neighboring utterances. This measure is typically labeled 'articulation rate'. Here we chose to refer to the more commonly used term 'speech rate', instead of 'articulation rate', for simplicity.

Stuttered-like disfluency (SLD) was defined as the percentage of part-word repetitions, monosyllabic-word repetitions and dysrhythmic phonations (including prolongations, blocks and broken words), out of the total number of syllables analyzed. Other disfluencies that are commonly found in fluent speakers (including interjections, revisions and multisyllabic/phrase repetitions) were not analyzed in the current study (Ambrose and Yairi 1999).

Stuttering severity evaluation

Stuttering severity was evaluated using the stuttering severity evaluation instrument (SSI-3) (Riley 1994). Following this protocol, we evaluated the percent of stuttered syllables, stuttering duration, and physical concomitants. The evaluation was obtained by two expert speech pathologists and was based on the audio and video recordings of the participants.

Statistical analysis

Due to the relatively small sample size, we could not rely on the assumption that the data is drawn from a specific probability distribution. Therefore, we used non-parametric statistics to analyze the data. To estimate group differences by means of age, gender, handedness, and education levels, the non-parametric Wilcoxon signed-rank test was used. Wilcoxon signed-rank test was further used to estimate group differences in speech rate. To evaluate the

association between speech rate and SLD we used Spearman's correlation.

Imaging data analysis

Software

Data analysis was conducted using Matlab 2012b (The Mathworks, Natick, MA). For data preprocessing, the open source 'mrDiffusion' package was used (https://github.com/vistalab/vistasoft/tree/master/mrDiffusion). Tract identification and quantification were implemented with the automatic fiber segmentation and quantification (AFQ) toolkit (Yeatman et al. 2012).

Data preprocessing

Diffusion MRI data were preprocessed in native space for each individual separately, following a published pipeline (Blecher et al. 2016; Kronfeld-Duenias et al. 2016a; Yablonski et al. 2018). This pipeline included a rigid transformation of the volume anatomy to the anterior commissure-posterior commissure (AC-PC) plane, motion- and eddy-current correction of DW-EPI data, alignment of DW-EPI data to the volume anatomy with the corresponding recalculation of the diffusion directions, resampling and tensor fitting. Specifically, T1 images were rotated to the AC-PC plane following manual identification of the anterior and posterior commissures. Diffusion weighted images were corrected for eddy-current and head motion distortions using a 14-parameter constrained non-linear co-registration algorithm based on the expected pattern of eddy-current distortions (Rohde et al. 2004). Additionally, each diffusion weighted image was registered to the mean of the two non-diffusion weighted (b0) images and the mean b0 image was registered automatically to the T1 image using a rigid body mutual information maximization algorithm (as implemented in SPM5; Friston and Ashburner 2004). The combined transform, incorporating both eddy-current correction and anatomical alignment, was applied to the raw diffusion data, and the diffusion data were resampled at $2\times2\times2$ cubic mm isotropic voxels. Gradient directions were adjusted according to the same transformation (Leemans and Jones 2009).

Diffusion tensors were fit to the registered diffusion data using a least-squares algorithm. Then, using tensor decomposition, we extracted the three eigenvectors and eigenvalues of the tensor, and calculated, for each voxel, fractional anisotropy (FA), mean diffusivity (MD), axial diffusivity (AD), and radial diffusivity (RD). FA was calculated as the normalized standard deviation of the eigenvalues. MD was calculated as the average of the three eigenvalues. AD was defined as the eigenvalue of the first eigenvector (diffusivity along the principal eigenvector). RD was defined as the average diffusivity of the second and third eigenvalues.

Tract identification and segmentation

We identified the three CPs bilaterally in each individual's native-space, resulting in six pathways for each participant: the left and right SCP, connecting the cerebellar nuclei with the contralateral thalamus; the left and right MCP, connecting the cerebrum with the contralateral cerebellar cortex via the pontine nuclei; and the left and right ICP, connecting the spine and the olivary nucleus with the ipsilateral cerebellar cortex (Fig. S1). To identify these tracts and quantify their diffusion parameters we used the AFQ package (Yeatman et al. 2012), which consists of the following steps: (1) whole-brain fiber tractography, (2) region-of-interest (ROI)-based tract segmentation and cleaning, and (3) quantification of diffusion parameters along the tract.

A whole-brain fiber group was tracked using a deterministic Streamlines Tractography (STT) algorithm (Basser et al. 2000; Mori et al. 1999) with a fourth-order Runge–Kutta path integration method and 1 mm fixed step size. To segment the tracts, we used a multiple waypoint-ROI approach in which the whole-brain fiber group was intersected with predefined waypoint-ROIs using logical operations. The waypoint-ROI was first defined on the JHU MNI T1 template and then back-transformed to each participant's native space (the specific location of the waypoint-ROIs can be found in Fig. S1). After tract segmentation, an automated cleaning procedure was applied to remove outlier streamlines from each individual's tract. Fibers were removed if they were longer than 1 standard deviation from the mean fiber length and spatially deviated more than 4 standard deviations from the core of the tract (Bruckert et al. 2019). Finally, diffusion properties were calculated at 30 equidistant nodes along the tract (Bruckert et al. 2019; Yeatman et al. 2012).

Manual ROI-definition of the CPs

To assess group differences reported in Connally et al. (2014), the CPs were defined once again as ROIs, without using tractography. This method was previously described in detail by Klein et al. (2011) and followed closely in Connally et al. (2014). In short, each tract was manually defined as a single ROI, placed in a pre-specified location on each peduncle, for a total of six ROIs per participant. For each ROI in each participant, diffusivity values (FA and MD) were averaged across all the voxels occupied by the ROI. Group comparisons were applied to these values as explained below.

Statistical analysis

Analyses were restricted to the core of the tracts, enclosed between the two waypoint-ROIs used for tractography. This approach eliminates the extreme segments of the tracts which are highly variable across participants.

Motion analysis We carried out head-motion analysis along the same protocol reported in Yendiki et al. (2014). In short, we computed three parameters for head motion (in voxels) and three parameters for rotation (in degrees) by registering each volume to the first volume. Then, we averaged the absolute values of each component over all the volumes for a given participant. A single translation component and a single rotation component were calculated for each participant, by averaging over the three parameters for each component. Finally, we compared each component (translation, rotation) between the groups using a *t*-test.

Group differences For each participant and each peduncle, we calculated the average FA and average MD value across the core of the tract (these values are termed tract-FA and tract-MD, respectively). These values were compared between the groups using the non-parametric Wilcoxon signed-rank test. Additionally, we evaluated local group-differences by comparing the local diffusivity measures in 30 nodes along each CP. This along-tract comparison typically provides better sensitivity compared to tract-FA and tract-MD comparisons, because the latter may mask group differences within systematic variability in diffusivity measures along the extent of the tract. To account for multiple comparisons, along-tract statistics were corrected using a non-parametric permutation test, controlling the family-wise error (FWE) corrected alpha at 0.05 (Nichols and Holmes 2002). To assess group differences within the ROI-defined CPs, we used a series of 6 Wilcoxon signed-rank tests (one per CP), FDR corrected at $p<0.05$. This non-parametric statistic was used to refrain from the assumption that the data is drawn from a predefined probability distribution. Power analysis revealed that a sample size of 19 participants in each group and significance of $\alpha=0.05$, is sufficient to obtain power of at least 0.83 for group differences in the SCP and ICP, and power of at least 0.64 in the MCP (based on the effect size reported in Connally et al. 2014).

Brain-behavior correlations Associations between the CPs and speech rate were assessed by calculating Spearman's rank-order correlations. First, we assessed the simple correlations between tract-FA and speech rate and between tract-MD and speech rate, for each CP. Second, to gain further sensitivity, we assessed the correlation of each peduncle with speech rate at 30 equidistant locations along the core of the tract (Yeatman et al. 2012). To account for multiple comparisons, significance was corrected using a non-parametric permutation test, controlling the family-wise error (FWE) corrected alpha at 0.05 (Nichols and Holmes 2002). To be considered a significant cluster of nodes, the cluster should have satisfied two criteria: (1) each node within the cluster was significantly correlated with speech rate at a level of alpha = 0.05 (uncorrected), and (2) the number of adjacent nodes composing the cluster should have been larger than a critical size, determined by the permutation algorithm (Nichols and Holmes 2002; Yeatman et al. 2012). Lastly, significant clusters were further examined by calculating the correlation between speech rate and the mean cluster AD or mean cluster RD.

Bayes factor analysis We measured the strength of evidence for group differences in white matter tracts by performing a Bayesian analysis. The analysis was carried out using the *ttestBF* function in the BayesFactor R package (Morey and Rouder 2018; R Core Team 2013). We restricted the Bayesian analysis to the mean-tract and ROI measurements to refrain from multiple comparisons along the tract.

Multiple linear regression To account for additional factors that could contribute to the results, we ran a multiple linear regression model. Specifically, we built a multiple linear regression model to predict speech rate by five different factors: (1) mean FA in the significant cluster of nodes; (2) SLD score; (3) age; (4) education; (5) written semantic fluency. To assess whether the effect of FA on speech rate is modified by SLD, we integrated into our model the interaction between FA and SLD. The analysis was carried out using the open-source R environment for statistical computing (R Core Team 2013).

Results

Two AWS participants were excluded from analysis, because they demonstrated extremely high SLDs (more than 4 SDs above the mean SLD of the AWS group). The demographic characteristics of the final analyzed sample ($N=42$) can be found in Table 1.

Behavioral results

The samples of AWS and controls were well matched in terms of age, gender, handedness, and education levels ($p>0.3$) (Table 1). As expected, the groups differed significantly in their stuttering severity scores, percent of stuttered-like syllables and speech rates, as indicated by a series of Wilcoxon signed-rank tests ($p<0.05$, see Table 1 and Fig. 1a). Spearman's correlation showed a significant negative correlation between speech rate and SLD in AWS,

Table 1 Sample characteristics and fluency measures[a]

	AWS ($N=23$)	Controls ($N=19$)	p
Age	31.17 [19–52]	33.26 [19–53]	n.s
Gender	6F/17 M	3F/16 M	n.s
Education	14.667 [12–21][b]	15.316 [12–21]	n.s
SSI-3	23 [10–41.5]	4.579 [2–10]	$*p=3.93\times10^{-8}$
SLD (%)	9.507 [3.09–23.82]	2.1794 [0.84–4.65]	$*p=1.47\times10^{-7}$
Speech rate (syllables/sec)	4.41 [2.06–6.61]	5.96 [4.56–7.02]	$*p=2.74\times10^{-4}$

AWS Adults who stutter, *SLD* stuttered-like-disfluencies per 100 syllables, *n.s.* not significant, *M* male, *F* female

$*p<0.05$

[a]The table depicts Mean [Range] values for each parameter, except Gender

[b]Education data are missing in two AWS, $N=21$

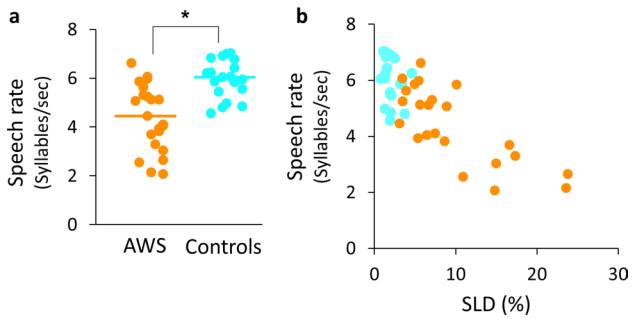

Fig. 1 Individual speech rates in AWS and controls. **a** Speech rate (in syllables per second) is presented for individuals in the AWS (orange) and control (cyan) groups. The median of each group is marked with a colored horizontal line. At the group level, speech rate in AWS is significantly smaller compared to controls ($p<0.001$). **b** In the AWS group (orange), a significant negative Spearman's correlation ($p<0.001$) is found between speech rate and SLD, indicating that more severe stuttering is associated with slower speech (recall that speech rate is assessed over fluent epochs only, so these measures are derived independently from the speech samples)

such that more frequent stuttering events were associated with slower speech ($r=-0.7213$, $p<0.0001$, Fig. 1b). The same analysis in the control group yielded a non-significant correlation ($r=-0.3053$, $p=0.2033$, Fig. 1b). Furthermore, Fisher's Z test confirmed that the correlation between speech rate and SLD observed in AWS was significantly different than the one observed in controls ($Z=-1.9530$, $p<0.05$).

Data quality control

The following steps were carried out as data quality control: First, we compared the head-motion parameters, between the groups (translation and rotation; see "Methods"), and found no significant group differences in these two parameters ($p>0.1$) (Fig. S2). Next, the 3D representation of the identified tracts were carefully examined by the first and last author (S.J & M.B-S) in every individual. Finally, we made sure that the automatic cleaning procedure (implemented in the AFQ package) removed a similar number of streamlines in both groups, AWS and controls (Fig. S3).

Identification of the cerebellar peduncles in individual participants

The bilateral SCP and MCP, and the left ICP were successfully identified in all participants ($N=42$). The right ICP was identified in 41 out of 42 participants but could not be identified in one control participant. Figure 2 shows the tracts of interest identified in six representative participants (three of each group).

No evidence for group differences in the microstructural properties of the CPs

FA and MD values were extracted from individual reconstructions of the CPs and compared between AWS and controls. First, we evaluated group differences in the mean tract-FA and tract-MD values of each tract. This analysis did not yield any significant group-differences in diffusivity values ($p>0.1$, FDR corrected for 6 comparisons for each dependent measure separately) (Tables S1 and S2). Recognizing that group-differences in FA and MD may be masked by averaging the diffusivity parameters along the trajectory of the pathway (Travis et. al. 2015), we further compared, node-by-node, the profiles of the diffusivity parameters along 30 equidistant nodes, in AWS vs. controls. This analysis, too, failed to detect any significant group-differences in the CPs ($p>0.1$, FDR corrected for 6 comparisons; See Fig. 3 for a visualization of FA profiles in each group and each CP, and Fig. S4 for a similar comparison of MD profiles). In fact, the profiles were so consistent between the

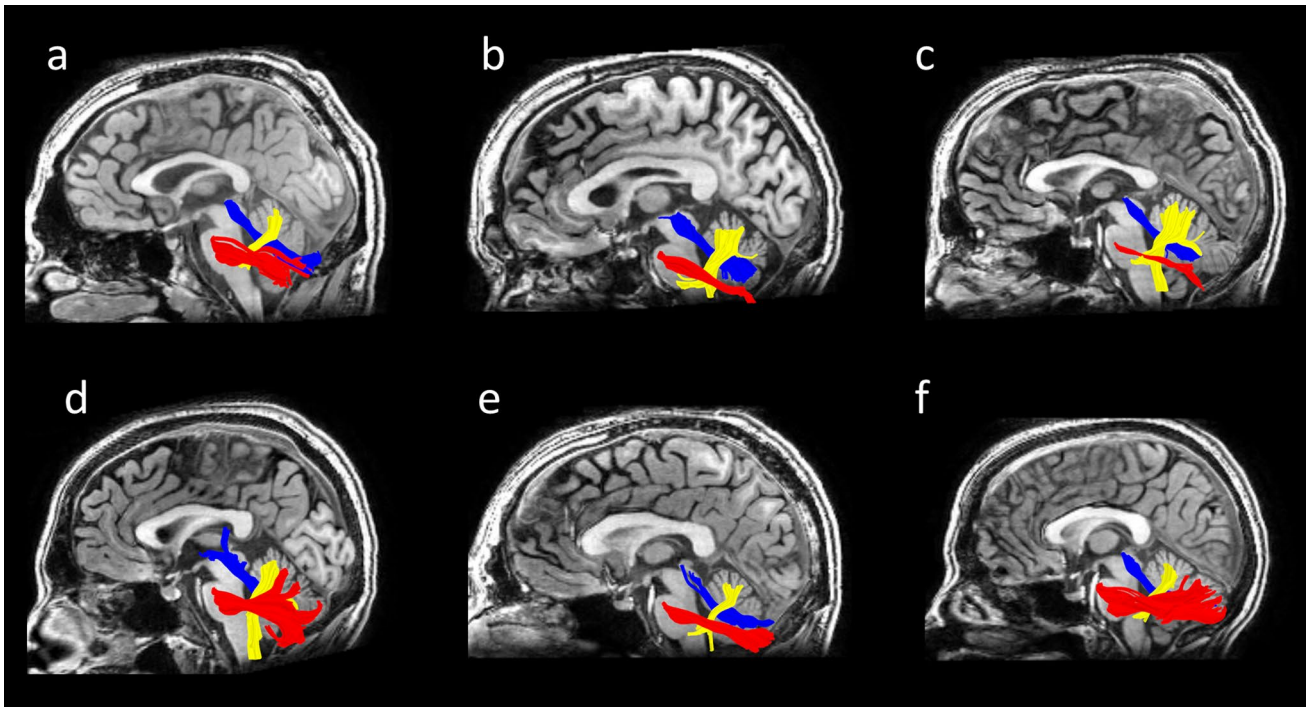

Fig. 2 Cerebellar peduncles in AWS and controls. Cerebellar peduncles of the left hemisphere are shown in six representative subjects. Tracts are overlaid on a midsagittal T1 image. (**a–c**) Three representative participants in the AWS group; (**d–f**) Three representative participants in the control group. Superior cerebellar peduncle (SCP; blue); Middle cerebellar peduncle (MCP; red); Inferior cerebellar peduncle (ICP; yellow)

groups, that they may be considered estimates of test–retest reliability of the measurements.

These results contradict findings from a previous study (Connally et al. 2014) that reported a significant FA reduction in the CPs of AWS compared to fluent speakers. A possible explanation for this discrepancy lies within the different methods used to define the CPs. In contrast to our tractography approach, Connally et al. (2014) used an ROI-based definition of the tracts. To test this possibility, we repeated the structural comparison between the groups, this time implementing the same analysis described in Connally et al. (2014) (Fig. 4; see "Methods" for details). This analysis, too, failed to detect any significant group differences in the CPs of AWS vs. controls (Fig. 5 and Fig. S5, and Tables S1 and S2). In summary, in the current sample, no significant group differences were detected in the CPs of AWS and controls, neither using tractography nor using anatomically defined ROIs.

A Bayesian analysis was further conducted to quantify the strength of evidence for white matter group differences. All Bayes factors were smaller than 1, providing support for the null hypothesis over the alternative hypothesis. A full description of the results is found in Tables S1 and S2.

Speech rate is associated with microstructural properties of the left ICP in AWS

To estimate the association between speech rate and the microstructural properties of the CPs, we first calculated Spearman's correlations between speech rate and mean tract diffusivities (tract-FA and tract-MD). These correlations were calculated for each peduncle and in each group separately (2 groups × 6 CPs × 2 diffusion parameters = 24 correlations overall). However, no significant correlation was detected between speech rate and mean tract diffusivities in the CPs ($p > 0.1$, uncorrected). To gain enhanced sensitivity for detecting localized brain-behavior correlations, we examined the associations between speech rate and local diffusivity values, node by node, along the trajectory of each cerebellar peduncle (see "Methods"). Using this analysis, we found a significant correlation in AWS between speech rate and FA within the left ICP ($r = -0.6235$, $p < 0.01$, FWE corrected across 30 nodes; see Fig. 6). Specifically, slower speech was associated with higher FA in a cluster of nodes within the left ICP (nodes 16–21). Moreover, the correlation coefficient in AWS differed significantly from the one calculated in corresponding nodes of the left ICP in control participants ($r = -0.0703$, Fisher's $Z = 1.763$, $p < 0.05$).

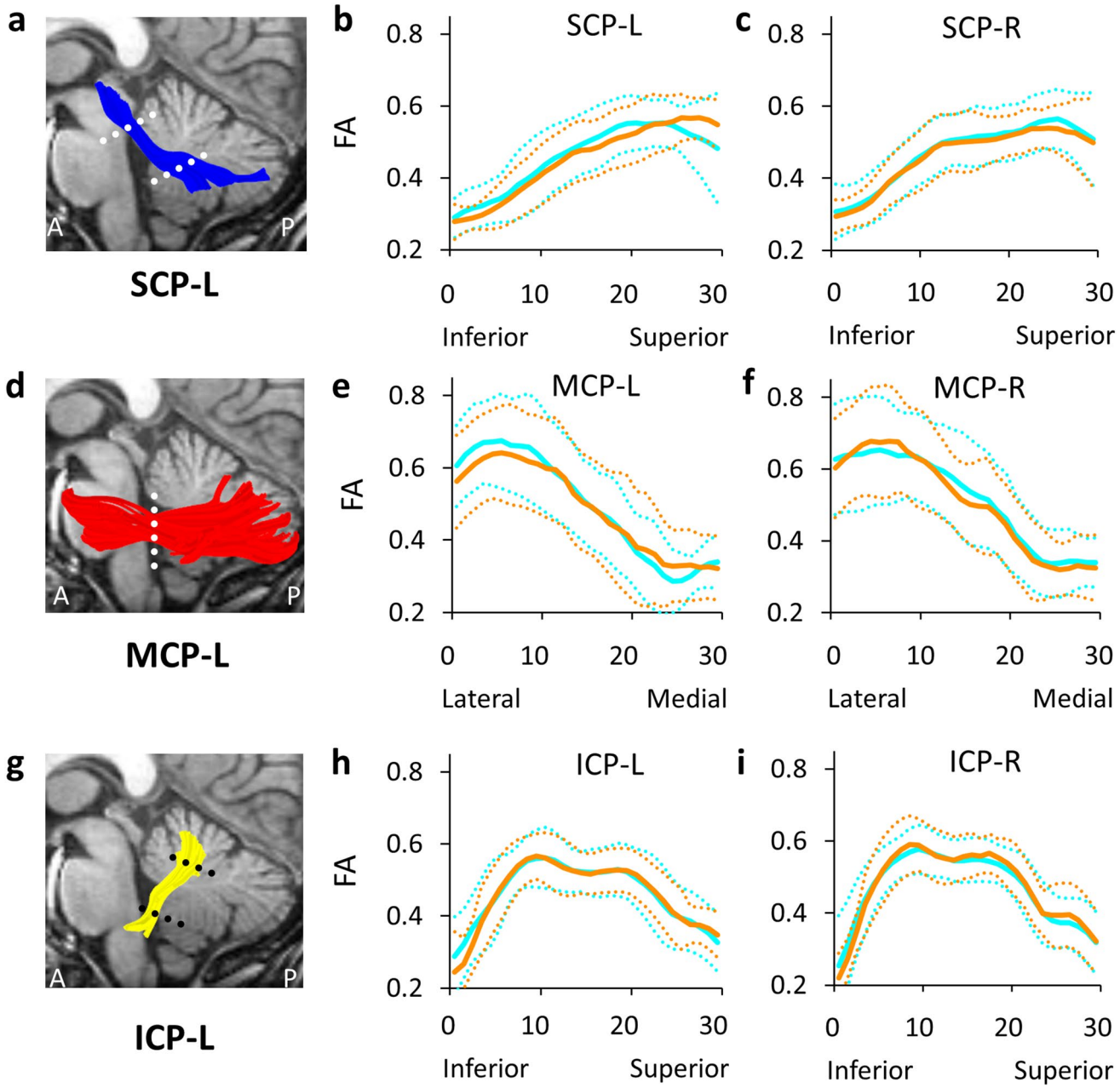

Fig. 3 Group comparison of FA profiles. The left SCP (**a**), MCP (**d**) and ICP (**g**) are visualized in a single control participant (male, 31), overlaid on a T1 image of the same participant. Dotted lines on the tractograms indicate the location of the waypoint-ROIs used for tract segmentation (see "Methods"). FA profiles are shown for the bilateral SCP (**b–c**), MCP (**e–f**) and ICP (**h–i**). The profiles are plotted along 30 equidistant nodes between two waypoint-ROIs. The colored lines indicate the average profile of AWS (orange) and controls (cyan). Colored dotted lines indicate ± 1 standard deviation for each group. *SCP-L* left superior cerebellar peduncle, *MCP-L* left middle cerebellar peduncle, *ICP-L* left inferior cerebellar peduncle, ROI- region of interest, *P* posterior, *A* anterior, *L* left, *R* right

A parallel analysis of MD tract-profiles in AWS did not detect any association with speech rate in any of the CPs. In controls, no significant correlations were found with speech rate in any of the CPs, considering both FA and MD as the dependent measure.

To further examine the microstructural factors underlying the association between the left ICP and speech rate in AWS, we calculated the mean-AD and mean-RD values within the cluster of nodes that showed a significant correlation with speech rate (nodes 16:21). A significant positive correlation was found between that cluster's mean-RD and speech rate ($r = 0.5148$, $p = 0.0119$). The correlation between speech rate and the mean-AD in this cluster was non-significant ($r = -0.3774$, $p = 0.0757$) (Fig. S6). In summary,

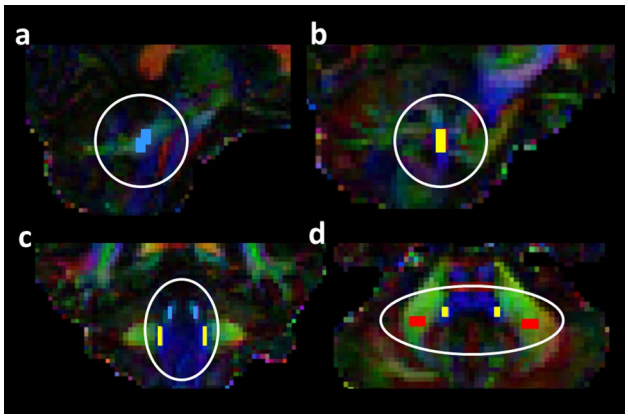

Fig. 4 CPs defined as ROIs. Following Fig. 4 in Connally et al. (2014), the 3 bilateral CPs were defined on participants' color-coded map depicting the principal diffusion direction (PDD) in each voxel. Voxels included in each ROI are shown here for a single control participant (male, 28). **a** The left SCP ROI is shown in light blue overlaid on a sagittal PDD map. **b** The left ICP ROI is shown in yellow overlaid on a sagittal PDD map. **c** The bilateral SCP (light blue) and ICP (yellow) ROIs are overlaid on a coronal view. **d** The bilateral MCP (red) and ICP (yellow) ROIs overlaid on an axial view

the association between FA and speech rate was primarily driven by RD in this cluster.

Finally, to account for additional factors that could contribute to the association between speech rate and white matter microstructure, we calculated a multiple linear regression model, predicting speech rate in AWS based on five factors: (1) mean FA in the significant cluster of nodes within the left ICP; (2) SLD score; (3) age; (4) education; (5) written semantic fluency. To assess whether the predictive effect of FA is modified by SLD, we further included in this model the interaction between FA and SLD. The results indicated that both FA and SLD, but not their interaction, contribute significantly to the prediction of speech rate (see Table 2). Age, education, and written semantic fluency did not contribute significantly to the model ($p > 0.1$).

Discussion

The current study aimed to assess microstructural differences in the cerebellar peduncles of AWS and controls, and to examine the potential associations between the CPs and speech rate in these two groups. Our data do not support previously reported group differences between AWS and fluent speakers in the microstructural properties of the CPs. However, we report differences between AWS and controls in the form of differential association patterns with speech rate within the left ICP. Specifically, we show that the microstructural properties of the left ICP, quantified with fractional anisotropy, are significantly correlated with speech rate in AWS, but not in controls, and this group difference was significant as assessed by the Fisher's *Z* test. Our results suggest that the left ICP is relevant for modulating speech rate in adults who have been stuttering for most of their lives. We discuss potential interpretations of these findings below.

No group differences in CP microstructure of AWS and controls

Contrary to previous findings by Connally et al. (2014), our data do not demonstrate group differences between AWS and fluent speakers in the microstructural properties of the CPs. We sought these differences in three different approaches, yet failed to find any significant group-difference, neither in a tractography-based definition of the CPs (comparing tract properties as tract-mean or along the tract), nor using an ROI definition of the CPs. The discrepancy between our results and previous findings could stem from several reasons, the most prominent ones relate to age and scan protocols, as we explain below.

Age: our sample spans an older group of participants compared to the previous sample (mean age: 31.2 years in our sample, compared to 22.6 years in Connally et al. 2014). This is particularly relevant: as shown in Connally et al. (2014), group differences in FA of the inferior cerebellar peduncle diminish dramatically with age (ibid., Fig. 5c). We, therefore, consider age the most likely reason for the differences observed in the pattern of results reported here compared to prior findings. A median split by age, however, failed to detect group differences even in our younger participants (Fig. S7). Still, a proper test of the age hypothesis would require a large scale cross-sectional dMRI study recruiting a sample of well-matched AWS and controls across a wide range of ages.

Scan protocol: different scanning protocols applied in each study could have an impact on the results. Connally et al. (2014) acquired dMRI data at higher angular resolution but relatively lower spatial resolution (60 gradient directions with a voxel size of 2.5 cubic mm). By comparison, our protocol combines lower angular resolution with a relatively higher spatial resolution (19 gradient directions scanned twice with a voxel size of 2 cubic mm). The trade-off between angular and spatial resolution may influence diffusion modeling at the voxel level (Schilling et al. 2017), potentially leading to different sensitivity to group differences.

What is the role of the ICP in mediating speech rate among AWS?

The ICP is a major cerebellar pathway, feeding signals from the olivary nucleus into the cerebellum via the climbing

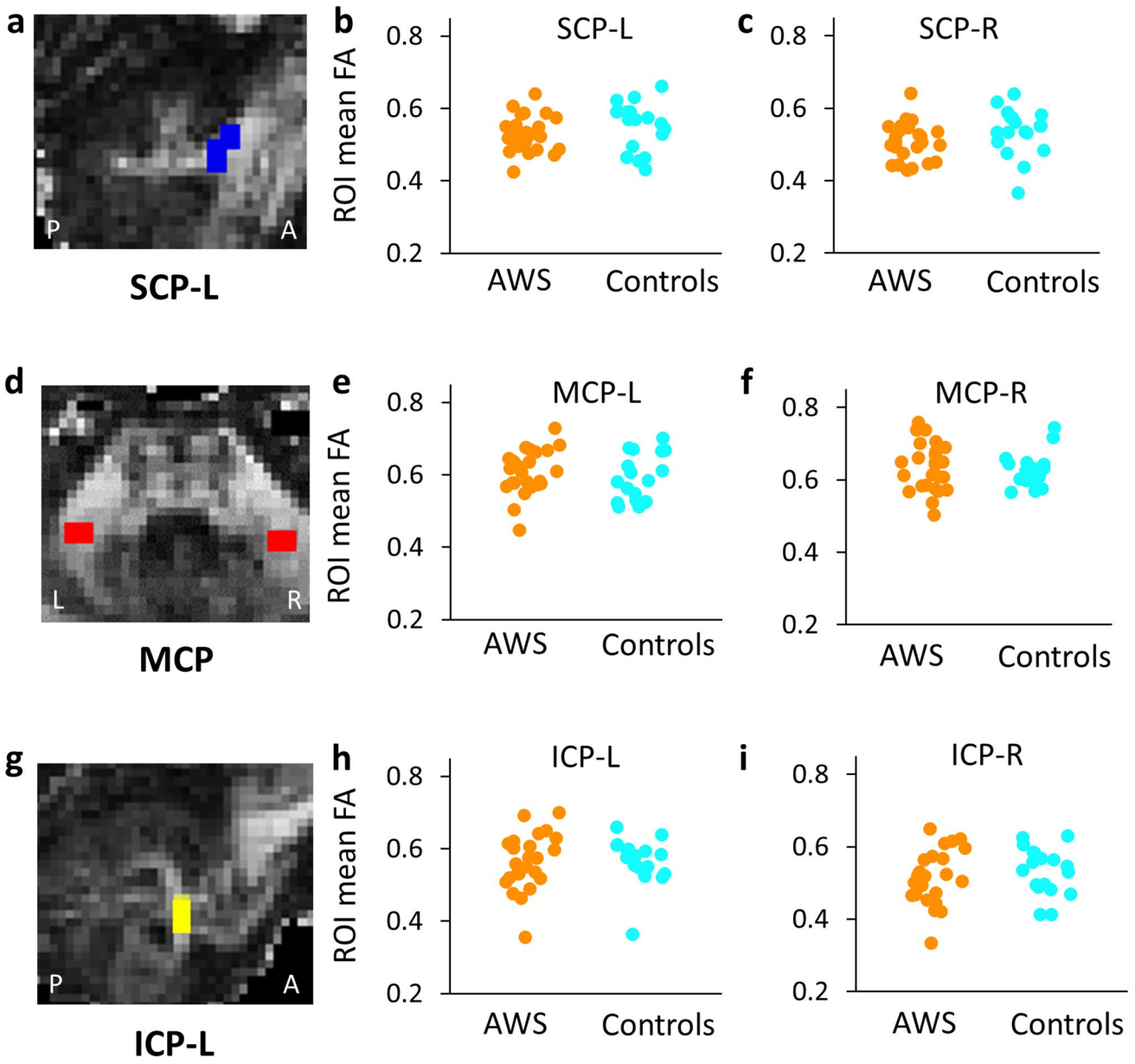

Fig. 5 Group comparison of FA in region-of-interest analysis. Data is shown for the SCP (panels **a–c**), MCP (panels **d–f**) and ICP (panels **g–i**). ROIs are visualized in a single control participant (male, 28) overlaid on the FA map (panels **a, d, g**). Mean FA extracted from the ROI of each participant is shown for the SCP (**b–c**), MCP (**e–f**) and ICP (**h–i**), bilaterally, for AWS (orange) and controls (cyan). *SCP* superior cerebellar peduncle, *MCP* middle cerebellar peduncle, *ICP* inferior cerebellar peduncle, *P* posterior, *A* anterior, *L* left, *R* right

fibers. These signals, transmitted through the olivo-cerebellar fibers, are repeatedly implicated in detecting motor errors (for review see Shadmehr 2017). The "error hypothesis" framework postulates that the inferior olive compares motor commands from the cerebrum with feedback from the periphery, thereby generating an error signal that is fed up to the cerebellum (Streng et al. 2018). This hypothesis has been supported in multiple motor behaviors, including locomotion (Andersson and Armstrong 1987; Jossinger et al. 2020), hand-reaching movements (Hewitt et al. 2015) and saccadic movements (Herzfeld et al. 2018).

Alterations in error monitoring during speech production have been proposed as part of the core deficit in stuttering (Arnstein et al. 2011; Max et al. 2004; Postma and Kolk 1993). One view of developmental stuttering suggests that AWS tend to over-rely on afferent feedback as a way to cope with an insufficient or unstable internal model of speech production (Max et al. 2004). Alternatively, other views

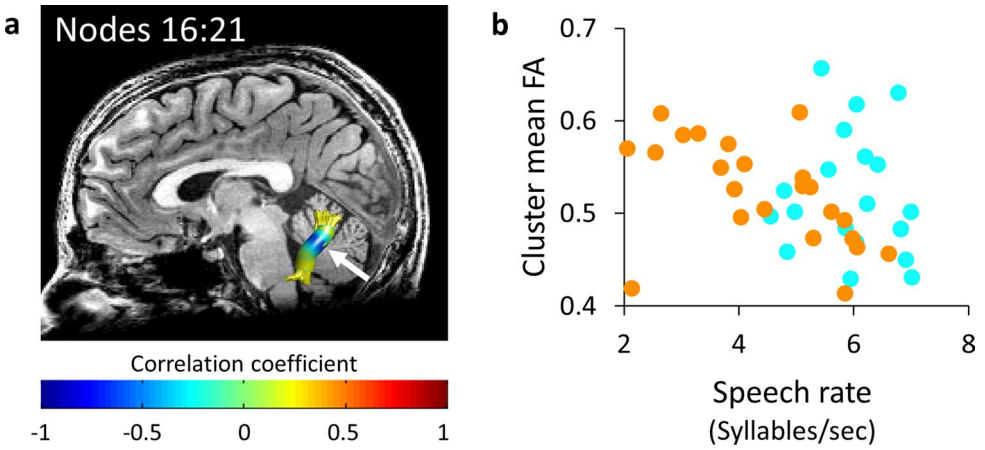

Fig. 6 Speech rate is correlated with white matter microstructure in the left ICP of adults who stutter, but not in controls. **a** The left ICP is shown in a single control participant (male, 31), overlaid on a mid-sagittal T1 image of the same individual. Colored overlay represents Spearman's *r* values between speech rate and FA in each node along the tract. The white arrow points to the significant cluster. **b** For each participant (AWS in orange, controls in cyan), the mean FA value of the significant cluster in panel **a** is plotted against the speech rate of the same individual

Table 2 Regression analysis for the prediction of speech rate (in AWS only, $N = 23$)

Factors	β	*t* value	*p*
FA[a]	− 23.97	− 2.59	0.022*
SLD (%)	− 0.64	− 2.408	0.031*
Age	− 0.03	− 0.839	0.416
Education	0.14	1.423	0.178
Semantic fluency (written)	0.02	0.425	0.677
FA × SLD (%)	1.00	1.890	0.08

*$p < 0.05$

[a]Mean FA in the significant cluster of L-ICP nodes, see Fig. 6 and accompanying text

postulate that the disfluencies in stuttering are due to hyperactive speech monitoring, where even minor deviations from the speech plan are considered as errors (Vasic and Wijnen 2005). This last view was supported by electrophysiological studies (Arnstein et al. 2011) as well as by computational models of speech (Civier et al. 2010). The superfluous correction and the low threshold for error detection may halt the fluent production of speech and lead to a reduction in speech rate in people who stutter.

Cerebellar implications in stuttering beyond speech rate

It is wildly accepted that the cerebellum is capable of generating "internal models" of the body's dynamics (Wolpert et al. 1998). According to the DIVA model (Guenther 2006), cerebellar internal models of speech production simulate the input–output relationships between the articulatory plan and its auditory consequence. If the actual auditory feedback does not fit the model's prediction, the sensorimotor system generates a corrective articulatory response to compensate for the acoustic error. Accumulative evidence suggests that stuttering may result in deficits in auditory-motor feedback monitoring, as AWS were shown to produce smaller corrective motor responses to compensate for auditory perturbations (Cai et al. 2012; Daliri et al. 2018). Recently, this deficit was also demonstrated in 3–9-year-old children who stutter, with a more prominent effect in the younger age group of 3–6 years (Kim et al. 2020). This suggests that impaired auditory-motor feedback monitoring during speech production may contribute to the onset of stuttering.

Theoretical models of stuttering suggest that the changes in speech rate, evident among people who stutter, are due to a disruption in a more general role of the cerebellum in timekeeping (Howell 2004; Ivry 1997). This theory is supported by clinical findings, showing that patients with damage to the cerebellum have impairments in behaviors that depend on accurate timing, including conditional learning (Raymond et al. 1996), agonist–antagonist muscle activity (Hore and Flament 1986), and speech production (Ackermann 2008). It is hypothesized that the cerebellar timekeeper marks the rate of ongoing events to enable the coordination between those events within a task. When interrupted, for example by increased load, the activities regulated by the cerebellar timekeeper are slowed (Howell 2004). In line with this view, the reduction in speech rate in persistent developmental stuttering can be attributed to low capacity of the timekeeping mechanism, which is unable to cope with an increasing rate of inputs.

Apart from timekeeping, the cerebellum has also been implicated in sensorimotor integration (Molinari et al. 2007). In this context, emerging data suggest that the overt impairment in timing among people who stutter results from a deficit in sensorimotor integration (Harrington et al. 2004; Iimura et al. 2019; Loucks and De Nil 2006). These views are supported by behavioral data showing that AWS demonstrate abnormal sensorimotor integration during jaw proprioception (Loucks and De Nil 2006), delayed auditory feedback task (Iimura et al. 2019), and even in a non-speech finger tapping task (Korzeczek et al. 2020; Loucks and De Nil 2006; Sares et al. 2019; Smits-Bandstra ans De Nil 2007). It is yet to be seen whether the cerebellum is directly involved in sensorimotor integration among AWS.

Unpacking a negative correlation with FA in terms of tissue properties

Our data show a negative correlation between speech rate and FA values within the left ICP of AWS, accompanied by a positive correlation with RD. That is, AWS who speak slower, on average, have higher FA values and lower RD values in the left ICP. FA is known to be affected by various biological factors including axonal diameter, axonal density, directional coherence, and myelin content (Assaf and Pasternak 2008; Beaulieu 2002; Jones et al. 2013). One potential explanation of our findings can be offered by focusing on myelin. It has been shown, on independent grounds, that FA is positively correlated with myelin water fraction (MWF) in core white matter areas (De Santis et al. 2014; Mädler et al. 2008; Stikov et al. 2015; Travis et al. 2019; Uddin et al. 2019). Since higher myelin content is related to faster conduction of information between neurons (Hartline and Colman 2007), we may carefully infer that higher FA may also be related to faster transfer of information. Along these lines, the negative correlation between FA and speech rate supports the hyperactive speech-monitoring hypothesis regarding AWS, suggesting that slower speech production in AWS is related to faster conduction of error signals through the ICP, which in turn reduces the fluent production of speech. This potential explanation, while speculative at this point, may be tested more directly in future measurements of myelin water fraction in the cerebellar pathways of AWS and fluent speakers.

Limitations

This study has several limitations. First, the relatively modest sample size ($N = 23$ for AWS and $N = 19$ for controls) limits the statistical power of our analysis. It is possible that larger samples would demonstrate significant group differences in the microstructural properties of the CPs. Second, our scan protocol was limited to a single shell measurement along 19 diffusion directions. This protocol enabled us to greatly reduce the scan duration, hence minimizing the within-scan head motion. To obtain an improved signal-to-noise ratio, we repeated the acquisition twice. While these scanning parameters are insufficient for fitting complex shapes such as constrained-spherical-convolution (CSD) (Tournier et al. 2008), they provide sufficient power for tensor fitting. In fact, it has been shown that using repeated scans (as used here) with six diffusion directions provides similar results as using a single scan of 30 directions (Lebel et al. 2012). This study still awaits replication with a more updated scanning protocol and analysis methods.

Finally, in a sample of adult participants, we cannot be conclusive about the direction of causality that underlies the correlation we detected in AWS. The observed correlation with speech rate in the left ICP may well reflect a compensation mechanism after years of rate-modification training, rather than the cause for slower speech in AWS. Studies in children who stutter are better suited to address the question of causality. Importantly, young children who stutter (aged 3–10 years) show modified functional and structural connectivity of the cerebellum compared with age-matched peers, suggesting an inherent deficit in cerebellar connectivity patterns in this population (Chang and Zhu 2013; Chang et al. 2015). Future intervention studies assessing the effect of speech rate modification on the CPs will provide the necessary evidence to address the question of causality.

Conclusions

In conclusion, the current study identifies, for the first time, an association between speech rate and the microstructural properties of the ICP in AWS. Furthermore, AWS and fluent speakers differ significantly in this correlation pattern. Thus, our findings support a role for the left ICP in modulating speech rate among AWS, but not in controls. By demonstrating the involvement of the ICP in developmental stuttering, our findings fit well within the view that stuttering stems from hyperactive speech monitoring, where even minor deviations from the speech plan are considered as errors (Vasic and Wijnen 2005). It remains to be seen whether the variability of the ICP among AWS reflects a compensatory mechanism, or rather a causal deficit that leads to a reduction in speech rate in this population.

Acknowledgements This study was conducted as part of Sivan Jossinger's doctoral dissertation, carried out under the supervision of Prof. Michal Ben-Shachar at the Gonda Multidisciplinary Brain Research Center, Bar-Ilan University. We thank the Israeli Stuttering Association (AMBI) for help with participant recruitment, and Dr. Ruth Ezrati-Vinacour for her involvement in the clinical evaluation of stuttering and her important contribution in earlier stages of this study. We also

thank the team at the Wohl institute for advanced imaging in Tel Aviv Sourasky Medical Center, for assistance with protocol setup and MRI scanning. We are grateful to Maya Yablonski and Galit Agmon for fruitful discussions. Finally, we thank Assaf Kindler for his support.

Funding This study is supported by the Israel Science Foundation (ISF Grant #1083/17).

Compliance with ethical standards

Conflict of interest The authors declare that there are no conflicts of interest.

References

Ackermann H (2008) Cerebellar contributions to speech production and speech perception: psycholinguistic and neurobiological perspectives. Trends Neurosci 31(6):265–272

Ackermann H, Brendel B (2016) Cerebellar contributions to speech and language. In: Neurobiology of language. Academic Press, pp 73–84

Adams M, Lewi J, Besozzi T (1973) The effect of reduced reading rate on stuttering frequency. J Speech Lang Hear Res 16(4):671–675

Alm PA (2004) Stuttering and the basal ganglia circuits: a critical review of possible relations. J Commun Disord 37(4):325–369

Ambrose NG, Yairi E (1999) Normative disfluency data for early childhood stuttering. J Speech Lang Hear Res JSLHR 42(4):895–909

Amir O (2016) Speaking rate among adult hebrew speakers: a preliminary observation. Ann Behav Sci 2(1):1–9

Amir O, Grinfeld D (2011) Articulation rate in childhood and adolescence: hebrew speakers. Lang Speech 54(2):225–240

Amir O, Levine-Yundof R (2013) Listeners' attitude toward people with dysphonia. J Voice 27(4):524.e1-524.e10

Andersson BYG, Armstrong DM (1987) Complex spikes in Purkinje cells in the lateral vermis (b zone) of the cat cerebellum during locomotion. J Physiol 385(1):107–134

Arnstein D, Lakey B, Compton RJ, Kleinow J (2011) Preverbal error-monitoring in stutterers and fluent speakers. Brain Lang 116(3):105–115

Assaf Y, Pasternak O (2008) Diffusion tensor imaging (DTI)-based white matter mapping in brain research: a review. J Mol Neurosci 34(1):51–61

Basser PJ, Pajevic S, Pierpaoli C, Duda J, Aldroubi A (2000) In vivo fiber tractography using DT-MRI data. Magn Reson Med 44(4):625–632

Beaulieu C (2002) The basis of anisotropic water diffusion in the nervous system: a technical review. NMR Biomed 15(7–8):435–455

Blecher T, Tal I, Ben-Shachar M (2016) White matter microstructural properties correlate with sensorimotor synchronization abilities. NeuroImage 138:1–12

Bohland JW, Guenther FH (2006) An fMRI investigation of syllable sequence production. NeuroImage 32(2):821–841

Bruckert L, Shpanskaya K, McKenna ES, Borchers LR, Yablonski M, Blecher T, Ben-Shachar M, Travis KE, Feldman HM, Yeom KW (2019) Age-dependent white matter characteristics of the cerebellar peduncles from infancy through adolescence. The Cerebellum 18(3):372–387

Cai S, Beal DS, Ghosh SS, Tiede MK, Guenther FH, Perkell JS (2012) Weak responses to auditory feedback perturbation during articulation in persons who stutter: evidence for abnormal auditory-motor transformation. PLoS ONE 7(7):1–13

Cai S, Tourville JA, Beal DS, Perkell JS, Guenther FH, Ghosh SS (2014) Diffusion imaging of cerebral white matter in persons who stutter: evidence for network-level anomalies. Front Hum Neurosci 8:1–18

Chang S-E, Zhu DC (2013) Neural network connectivity differences in children who stutter. Brain 136(12):3709–3726

Chang SE, Erickson KI, Ambrose NG, Hasegawa-Johnson MA, Ludlow CL (2008) Brain anatomy differences in childhood stuttering. Neuroimage 39(3):1333–1344

Chang S-E, Horwitz B, Ostuni J, Reynolds R, Ludlow CL (2011) Evidence of left inferior frontal-premotor structural and functional connectivity deficits in adults who stutter. Cereb Cortex 21(11):2507–2518

Chang S-E, Zhu DC, Choo AL, Angstadt M (2015) White matter neuroanatomical differences in young children who stutter. Brain 138(3):694–711

Cieslak M, Ingham RJ, Ingham JC, Grafton ST (2015) Anomalous white matter morphology in adults who stutter. J Speech Lang Hear Res 58(2):268–277

Civier O, Tasko SM, Guenther FH (2010) Overreliance on auditory feedback may lead to sound/syllable repetitions: simulations of stuttering and fluency-inducing conditions with a neural model of speech production. J Fluen Disord 35(3):246–279

Connally EL, Ward D, Howell P, Watkins KE (2014) Disrupted white matter in language and motor tracts in developmental stuttering. Brain Lang 131:25–35

Daliri A, Wieland EA, Cai S, Guenther FH, Chang S-E (2018) Auditory-motor adaptation is reduced in adults who stutter but not in children who stutter. Dev Sci 21(2):e12521

de Andrade CRF, Cervone LM, Sassi FC (2003) Relationship between the stuttering severity index and speech rate. Sao Paulo Medical Journal = Revista Paulista de Medicina 121(2):81–84

De Nil LF, Kroll RM, Lafaille SJ, Houle S (2003) A positron emission tomography study of short-and long-term treatment effects on functional brain activation in adults who stutter. J Fluen Disord 28(4):357–380

De Santis S, Drakesmith M, Bells S, Assaf Y, Jones DK (2014) Why diffusion tensor MRI does well only some of the time: Variance and covariance of white matter tissue microstructure attributes in the living human brain. NeuroImage 89:35–44

Dietz V, Zijlstra W, Duysens J (1994) Human neuronal interlimb coordination during split-belt locomotion. Exp Brain Res 101(3):513–520

Fox P, Ingham R, Ingham J, Zamarripa F, Xiong J, Lancaster J (2000) Brain correlates of stuttering and syllable production. A PET performance-correlation analysis. Brain 123(10):1985–2004

Friston KJ, Ashburner J (2004) Generative and recognition models for neuroanatomy. NeuroImage 23(1):21–24

Guenther FH (2006) Cortical interactions underlying the production of speech sounds. J Commun Disord 39(5):350–365

Halag-Milo T, Stoppelman N, Kronfeld-Duenias V, Civier O, Amir O, Ezrati-Vinacour R, Ben-Shachar M (2016) Beyond production: brain responses during speech perception in adults who stutter. NeuroImage Clin 11:328–338

Hall KD, Amir O, Yairi E (1999) A longitudinal investigation of speaking rate in preschool children who stutter. J Speech Lang Hear Res 42(6):1367–1377

Harrington DL, Lee RR, Boyd LA, Rapcsak SZ, Knight RT (2004) Does the representation of time depend on the cerebellum? effect of cerebellar stroke. Brain 127(3):561–574

Hartline DK, Colman DR (2007) Rapid conduction and the evolution of giant axons and myelinated fibers. Curr Biol 17(1):29–35

Herzfeld DJ, Kojima Y, Soetedjo R, Shadmehr R (2018) Encoding of error and learning to correct that error by the Purkinje cells of the cerebellum. Nat Neurosci 21(5):736–743
Hewitt AL, Popa LS, Ebner TJ (2015) Changes in Purkinje cell simple spike encoding of reach kinematics during adaption to a mechanical perturbation. J Neurosci 35(3):1106–1124
Hickok G (2012) Computatinal neuroanatomy of speech production. Nat Rev Neurosci 13(2):135–145
Hore J, Flament D (1986) Evidence that a disordered servo-like mechanism contributes to tremor in movements during cerebellar dysfunction. J Neurophysiol 56:123–136
Howell P (2004) Assessment of some contemporary theories of stuttering that apply to spontaneous speech. Contemp Issues Commun Sci Disord CICSD 31:122–139
Iimura D, Asakura N, Sasaoka T, Inui T (2019) Abnormal sensorimotor integration in adults who stutter: A behavioral study by adaptation of delayed auditory feedback. Front Psychol 10:1–11
Ingham RJ, Grafton ST, Bothe AK, Ingham JC (2012) Brain activity in adults who stutter: similarities across speaking tasks and correlations with stuttering frequency and speaking rate. Brain Lang 122(1):11–24
Ivry R (1997) Cerebellar timing systems. Int Rev Neurobiol 41:555–573
Jones DK, Knösche TR, Turner R (2013) White matter integrity, fiber count, and other fallacies: the do's and don'ts of diffusion MRI. NeuroImage 73:239–254
Jossinger S, Mawase F, Ben-Shachar M, Shmuelof L (2020) Locomotor adaptation is associated with microstructural properties of the inferior cerebellar peduncle. The Cerebellum 19(3):370–382
Kavé G (2005) Standardization and norms for a Hebrew naming test. Brain Lang 92(2):204–211
Kell CA, Neumann K, von Kriegstein K, Posenenske C, von Gudenberg AW, Euler H, Giraud A (2009) How the brain repairs stuttering. Brain 132(10):2747–2760
Kemerdere R, de Champfleur NM, Deverdun J, Cochereau J, Moritz-Gasser S, Herbet G, Duffau H (2016) Role of the left frontal aslant tract in stuttering: a brain stimulation and tractographic study. J Neurol 263(1):157–167
Kent RD, Rosenbek JC (1983) Acoustic patterns of apraxia of speech. J Speech Lang Hear Res 26(2):231–249
Kent RD, Kent JF, Rosenbek JC (1987) Maximum performance tests of speech production. J Speech Hear Disord 52(4):367–387
Kim KS, Daliri A, Flanagan JR, Max L (2020) Dissociated development of speech and limb sensorimotor learning in stuttering: speech auditory-motor learning is impaired in both children and adults who stutter. Neuroscience 451:1–21
Klein JC, Lorenz B, Kang J-S, Baudrexel S, Seifried C, van de Loo S, Steinmetz H, Deichmann R, Hilker R (2011) Diffusion tensor imaging of white matter involvement in essential tremor. Hum Brain Mapp 32(6):896–904
Kloth SAM, Janssen P, Kraaimaat FW, Brutten GJ (1995) Speech-motor and linguistic skills of young stutterers prior to onset. J Fluen Disord 20(2):157–170
Korzeczek A, Cholin J, Jorschick A, Hewitt M, Sommer M (2020) Finger sequence learning in adults who stutter. Front Psychol 11(July):1–12
Kronfeld-Duenias V, Amir O, Ezrati-Vinacour R, Civier O, Ben-Shachar M (2016a) The frontal aslant tract underlies speech fluency in persistent developmental stuttering. Brain Struct Funct 221(1):365–381
Kronfeld-Duenias V, Amir O, Ezrati-Vinacour R, Civier O, Ben-Shachar M (2016b) Dorsal and ventral language pathways in persistent developmental stuttering. Cortex 81:79–92
Kronfeld-Duenias V, Civier O, Amir O, Ezrati-Vinacour R, Ben-Shachar M (2018) White matter pathways in persistent developmental stuttering: Lessons from tractography. J Fluen Disord 55:68–83
Lebel C, Benner T, Beaulieu C (2012) Six is enough? Comparison of diffusion parameters measured using six or more diffusion-encoding gradient directions with deterministic tractography. Magn Reson Med 68(2):474–483
Leemans A, Jones DK (2009) The B -matrix must be rotated when correcting for subject motion in DTI data. Magn Reson Med 61(6):1336–1349
Loucks TMJ, De Nil LF (2006) Anomalous sensorimotor integration in adults who stutter: a tendon vibration study. Neurosci Lett 402(1–2):195–200
Lu C, Ning N, Peng D, Ding G, Li K, Yang Y, Lin C (2009) The role of large-scale neural interactions for developmental stuttering. Neuroscience 161(4):1008–1026
Lu C, Chen C, Peng D, You W, Zhang X, Ding G, Deng X, Yan Q, Howell P (2012) Neural anomaly and reorganization in speakers who stutter: a short-term intervention study. Neurology 79(7):625–632
Mädler B, Drabycz SA, Kolind SH, Whittall KP, MacKay AL (2008) Is diffusion anisotropy an accurate monitor of myelination? Magn Reson Imaging 26(7):874–888
Max L, Guenther F, Gracco V (2004) Unstable or insufficiently activated internal models and feedback-biased motor control as sources of dysfluency: a theoretical model of stuttering. Contemp Issues Commun Sci Disord 31:105–122
Molinari M, Leggio MG, Thaut MH (2007) The cerebellum and neural networks for rhythmic sensorimotor synchronization in the human brain. Cerebellum 6(1):18–23
Morey RD, Rouder JN (2018) BayesFactor: computation of Bayes factors for common designs. R package version 0.9.12-4.2. https://CRAN.R-project.org/package=BayesFactor
Mori S, Crain BJ, Chacko VP, Van Zijl PCM (1999) Three-dimensional tracking of axonal projections in the brain by magnetic resonance imaging. Ann Neurol 45(2):265–269
Neef NE, Anwander A, Bütfering C, Schmidt-Samoa C, Friederici AD, Paulus W, Sommer M (2018) Structural connectivity of right frontal hyperactive areas scales with stuttering severity. Brain 141(1):191–204
Nichols TE, Holmes AP (2002) Nonparametric permutation tests for functional neuroimaging: a primer with examples. Hum Brain Mapp 15(1):1–25
Perrini P, Tiezzi G, Castagna M, Vannozzi R (2013) Three-dimensional microsurgical anatomy of cerebellar peduncles. Neurosurg Rev 36(2):215–225
Postma A, Kolk H (1993) The covert repair hypothesis: prearticulatory repair processes in normal and stuttered disfluencies. J Speech Hear Res 36(3):472–487
R Core Team (2013) R: A language and environment for statistical computing. R Foundation for Statistical Computing, Vienna
Raymond J, Lisberger S, Mauk M (1996) The cerebellum: a neuronal learning machine? Science 272(5265):1126–1131
Riecker A, Mathiak K, Wildgruber D, Erb M, Hertrich I, Grodd W, Ackermann H (2005) fMRI reveals two distinct cerebral networks subserving speech motor control. Neurology 64(4):700–706
Riecker A, Kassubek J, Gröschel K, Grodd W, Ackermann H (2006) The cerebral control of speech tempo: opposite relationship between speaking rate and BOLD signal changes at striatal and cerebellar structures. NeuroImage 29(1):46–53
Riley G (1994) Stuttering severity instrument for children and adults, 3rd edn. Pro-Ed, Austin, Texas
Rochman D, Amir O (2013) Examining in-session expressions of emotions with speech/vocal acoustic measures: an introductory guide. Psychother Res 23(4):381–393

Rohde GK, Barnett AS, Basser PJ, Marenco S, Pierpaoli C (2004) Comprehensive approach for correction of motion and distortion in diffusion-weighted MRI. Magn Reson Med 51(1):103–114

Sares AG, Deroche MLD, Shiller DM, Gracco VL (2019) Adults who stutter and metronome synchronization: evidence for a nonspeech timing deficit. Ann NY Acad Sci 1449(1):56–69

Schalling E, Hartelius L (2013) Speech in spinocerebellar ataxia. Brain Lang 127(3):317–322

Schilling K, Gao Y, Janve V, Stepniewska I, Landman BA, Anderson AW (2017) Can increased spatial resolution solve the crossing fiber problem for diffusion MRI? NMR Biomed 30(12):e3787

Shadmehr R (2017) Learning to predict and control the physics of our movements. J Neurosci 37(7):1663–1671

Sitek KR, Cai S, Beal DS, Perkell JS, Guenther FH, Ghosh SS (2016) Decreased cerebellar-orbitofrontal connectivity correlates with stuttering severity: whole-brain functional and structural connectivity associations with persistent developmental stuttering. Front Hum Neurosci 10(MAY2016):1–11

Smits-Bandstra S, De Nil LF (2007) Sequence skill learning in persons who stutter: implications for cortico-striato-thalamo-cortical dysfunction. J Fluen Disord 32(4):251–278

Stikov N, Campbell JSW, Stroh T, Lavelée M, Frey S, Novek J, Nuara S, Ho MK, Bedell BJ, Dougherty RF, Leppert IR, Boudreau M, Narayanan S, Duval T, Cohen-Adad J, Picard PA, Gasecka A, Côté D, Pike GB (2015) In vivo histology of the myelin g-ratio with magnetic resonance imaging. NeuroImage 118:397–405

Streng ML, Popa LS, Ebner TJ (2018) Complex spike wars: a new hope. The Cerebellum 17(6):735–746

Tournier JD, Yeh CH, Calamante F, Cho KH, Connelly A, Lin CP (2008) Resolving crossing fibres using constrained spherical deconvolution: validation using diffusion-weighted imaging phantom data. NeuroImage 42(2):617–625

Tourville JA, Guenther FH (2013) DIVA model for speech acquisition. Lang Cogn Process 26(7):1–27

Travis KE, Leitner Y, Feldman HM, Ben-Shachar M (2015) Cerebellar white matter pathways are associated with reading skills in children and adolescents. Hum Brain Mapp 36(4):1536–1553

Travis KE, Castro MRH, Berman S, Dodson CK, Mezer AA, Ben-Shachar M, Feldman HM (2019) More than myelin: probing white matter differences in prematurity with quantitative T1 and diffusion MRI. NeuroImage Clin 22:101756

Tremblay P, Deschamps I, Gracco VL (2016) Neurobiology of speech production: a motor control perspective. In: Neurobiology of language. Academic Press, pp 741–750

Uddin MN, Figley TD, Solar KG, Shatil AS, Figley CR (2019) Comparisons between multi-component myelin water fraction, T1w/T2w ratio, and diffusion tensor imaging measures in healthy human brain structures. Sci Rep 9(1):2500

Vasic N, Wijnen F (2005) Stuttering as a monitoring deficit. In: Hartsuiker RJ, Bastiaanse R, Postma A, Wijnen F (eds) Phonological encoding and monitoring in normal and pathological speech. Psychology Press, pp 226–247

Watkins KE, Smith SM, Davis S, Howell P (2007) Structural and functional abnormalities of the motor system in developmental stuttering. Brain 131(1):50–59

Watkins K, Chesters J, Connally E (2015) The neurobiology of developmental stuttering. In: Hickok G SS (ed) Neurobiology of language. Elsevier, Amsterdam, pp 995–1004

Wolpert DM, Miall RC, Kawato M (1998) Internal models in the cerebellum. Trends Cogn Sci 2(9):338–347

Xuan Y, Meng C, Yang Y, Zhu C, Wang L, Yan Q, Lin C, Yu C (2012) Resting-state brain activity in adult males who stutter. PLoS ONE 7(1):e30570

Yablonski M, Rastle K, Taylor JSH, Ben-Shachar M (2018) Structural properties of the ventral reading pathways are associated with morphological processing in adult English readers. Cortex 116:1–18

Yang Y, Jia F, Siok WT, Tan LH (2016) Altered functional connectivity in persistent developmental stuttering. Sci Rep 6(1):19128

Yeatman JD, Dougherty RF, Myall NJ, Wandell BA, Feldman HM (2012) Tract profiles of white matter properties: automating fiber-tract quantification. PLoS ONE 7(11):e49790

Yendiki A, Koldewyn K, Kakunoori S, Kanwisher N, Fischl B (2014) Spurious group differences due to head motion in a diffusion MRI study. NeuroImage 88:79–90

Zimmermann G (1980a) Articulatory behaviors associated with stuttering. J Speech Lang Hear Res 23(1):108–121

Zimmermann G (1980b) Articulatory dynamics of fluent utterances of stutterers and nonstutterers. J Speech Lang Hear Res 23(1):95–107

Zimmermann G (1980c) Stuttering. J Speech Lang Hear Res 23(1):122–136